

CrossMark
click for updates

Cite this: DOI: 10.1039/c4nj02372b

Nickel nanoparticles assisted regioselective synthesis of pyrazoloquinolinone and triazoloquinazolinone derivatives†

Nongthombam Geetmani Singh,^a Rammamorthy Nagarajaprakash,^b Jims World Star Rani,^a Chingrishon Kathing,^a Ridaphun Nongrum^a and Rishanlang Nongkhlaw^{*a}

Received (in Montpellier, France)
22nd December 2014,
Accepted 24th February 2015

DOI: 10.1039/c4nj02372b

www.rsc.org/njc

Biologically important pyrazoloquinolinone and triazoloquinazolinone derivatives were synthesized by the condensation reaction of 3-amino-1*H*-1,2,4-triazole/3-amino-5-methyl-1*H*-pyrazole, dimedone and aryl aldehydes using catalytic amount of magnetically retrievable nickel nanoparticles under reflux condition. This protocol eliminates the usage of toxic reagents, complex work-up conditions, etc., with the added benefit of reusability of the catalyst without compromising the yield or purity of the product.

Introduction

Metal nanocatalysis has emerged as a novel strategy for the syntheses of diverse organic molecules, and its application in various organic transformations¹ as a heterogeneous catalyst is remarkable. The synthetic utility of nanocatalysts derived from Ag, Au, Ni, Fe, Pd, Cu, Fe₂O₃, NiO, etc. has become an intriguing topic of discussion within the research fraternity.

Synthetic studies on heterocycles have been evolving since time immemorial and in this present decade of nanotechnology, researchers are trying to harvest the potential possessed by nanoparticles to various extents. Amongst nanocatalysts, nickel nanoparticles have emerged as potent eco-friendly catalysts owing to their unique recyclability properties which allow them to be retrieved with ease by using a simple magnet after completion of a reaction and then reused multiple times without compromising the yield of the desired products. This has been exploited for the chemo-selective oxidative coupling of thiols,² the hydrothermal Heck reaction,³ α -alkylation of methyl ketones,⁴ reduction of aldehydes and ketones,^{5a-c} the transfer hydrogenation reaction,⁶ simple olefin hydrogenation,⁷ Wittig-type olefination for the synthesis of stilbenes from alcohol⁸ and as supports for hydrogen adsorption.⁹

Nanocatalysis of multicomponent reactions (MCRs) has also become considerably important these days due to its strategic advantages over conventional synthetic methods.¹⁰ MCR minimizes

the unnecessary wastage of chemicals, resources and time. Synthesis of N-heterocycles by MCR methods has been the prime target of synthetic chemists, since nitrogen containing moieties form an integral part of many biologically active molecules and natural products. Triazoloquinazolinone in particular, has established itself as an important therapeutic agent¹¹ and has found multiple applications as an anti-HIV,¹² analgesic,¹³ antihypertensive,¹⁴ anti-histaminic,¹⁵ antitumour¹⁶ and anticancer¹⁷ agent, etc. Many research groups have reported its synthesis using different conventional and non-conventional¹⁸ methods. They used either silica gel,¹⁹ molecular iodine,²⁰ H₆P₂W₁₈O₆₂·18H₂O²¹ or hydrotalcites,²² etc.

Another class of nitrogen heterocycle, *i.e.* pyrazolo[3,4-*b*]quinolines, has emerged as an important pharmaceutical entity due to their parasiticidal,²³ bactericidal,²⁴ antiviral²⁵ and antimalarial²⁶ properties. They have also found application as vasodilators²⁷ and has been extensively studied for their enzyme inhibiting activity.²⁸

All the reported syntheses of triazoloquinazolinone and pyrazoloquinolinone derivatives encountered certain drawbacks, such as the use of expensive catalysts, long reaction time, toxic reaction conditions, purification complications, low yield, etc. According to our survey no literature has been reported on the synthesis of triazoloquinazolinones and pyrazoloquinolinones using nanoparticles. Moreover, the necessity to develop a catalyst which can be reused after recycling by simple methods led us to the development of a novel protocol involving the use of magnetically retrievable nickel nanoparticles (Fig. 1).

Results and discussion

Our present work deals with the synthesis of triazoloquinazolinones/pyrazoloquinolinones through a simple method in

^a Centre for Advanced Studies in Chemistry, North Eastern Hill University, Shillong-793022, India. E-mail: rlnongkhlaw@nehu.ac.in; Fax: +91-364-2550076; Tel: +91-364-2722628

^b Department of Chemistry, Pondicherry University, Puducherry 605014, India

† Electronic supplementary information (ESI) available. CCDC 1024256 and 1024257. For ESI and crystallographic data in CIF or other electronic format see DOI: 10.1039/c4nj02372b

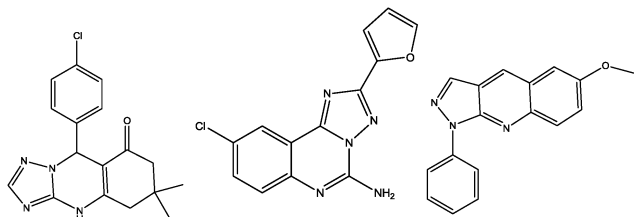


Fig. 1 Some biologically important triazoloquinazolinones and pyrazoloquinolinones.

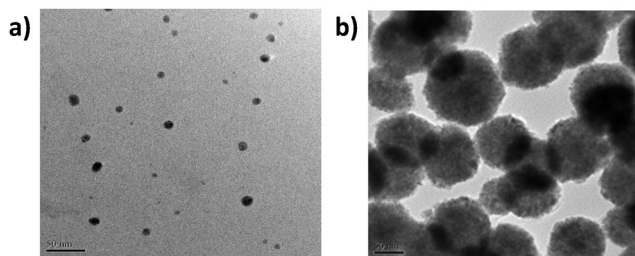
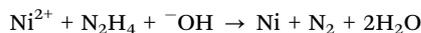


Fig. 2 TEM image of Ni NPs: (a) before use (b) after 6 runs.

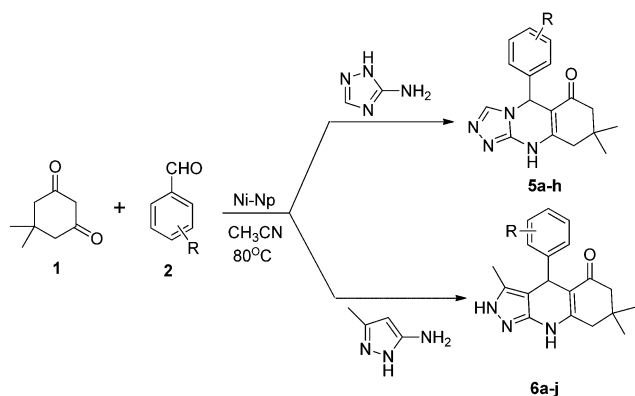
which the reactants, 3-amino-1*H*-1,2,4-triazole/3-amino-5-methyl-1*H*-pyrazole (1 mmol), aldehyde (1 mmol) and dione (1 mmol) were refluxed in acetonitrile. Instead of using a base or an acid catalyst, we decided on using nickel nanoparticles as catalyst and study the multi-component reaction (Scheme 1).

Catalyst preparation and characterization

The nickel nanoparticles were prepared as reported²⁹ by chemical reduction of nickel chloride hexahydrate with hydrazine hydrate at room temperature without using any protective agent or inert gas protection.



The nickel nanoparticles were retrieved magnetically and reused several times. The time taken for completion of reaction was 10 minutes, and the product was recovered in pure form as crystals on cooling. When the reaction was carried out under solvent-free conditions, the desired product was not obtained.



Scheme 1 Proposed scheme for the synthesis of various triazoloquinazolinone and pyrazoloquinolinone derivatives.

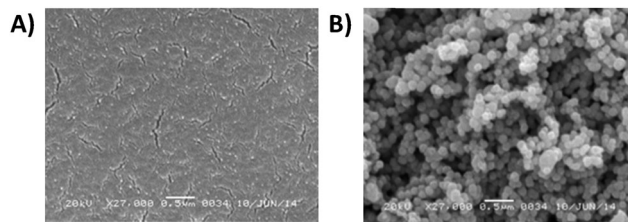


Fig. 3 SEM image of Ni NPs: (A) before use (B) after 6 runs.

Similarly, when other organic solvents such as ethanol, methanol, dichloromethane, *etc.* were employed, a negligible yield or no yield was obtained. The nickel nanoparticles were characterized by scanning electron microscopy (SEM), transmission electron microscopy (TEM), energy-dispersive X-ray (EDAX) and powder XRD (Fig. 3).

As we can see from the images, the size of the nanoparticles varied from 2–12 nm before being implemented as a catalyst. A histogram diagram of the synthesized nickel nanoparticles is shown in Fig. 4. However, after the sixth cycle, the nanoparticles seem to have aggregated to give particles of size 50 nm and above.

Further, in order to dispense any doubts regarding the oxidation of the nickel nanoparticles by air to nickel oxides, we performed EDAX and powder XRD analysis on the synthesized nanoparticles. The EDAX spectrum (Fig. 5) show no traces of oxygen moieties and the nanoparticles appear to be comprised of nickel only.

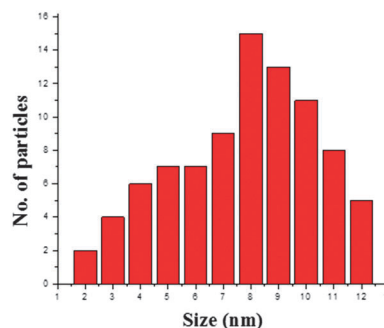


Fig. 4 Histogram diagram of Ni NPs.

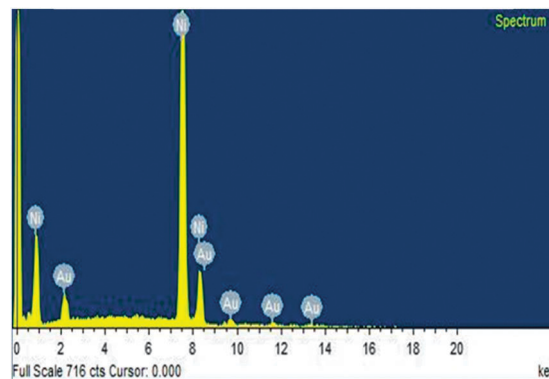


Fig. 5 EDAX of prepared nickel nanoparticle.

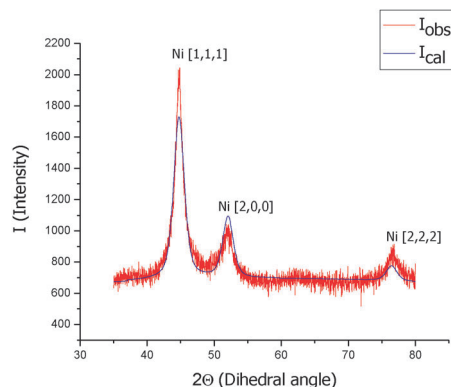


Fig. 6 Powder XRD pattern of Ni(O) nanoparticles.

Moreover, the strong magnetic attraction exhibited by our nanoparticles confirmed that it is not antiferromagnetic and so dispelled any uncertainty of it being NiO.

The powder XRD pattern of the nickel nanoparticles (Fig. 6) displayed characteristic dihedral angles at 44.87° , 51.79° and 76.81° , corresponding to nickel(0) nanoparticles.

The above characterized nanoparticles were then employed for the synthesis of **5a–h** and **6a–j**. Due to the presence of three non-equivalent nucleophilic centers *i.e.* N2, C4 and NH₂, *etc.*, in the aminopyrazole building block unit, reactions of 3-aminopyrazoles with cyclic 1,3-diketones and aromatic aldehydes may lead to different tricyclic products. Thus, such kind of reactions can generate mixtures of pyrazoloquinolinones (Hantzsch-type product) and pyrazoloquinazolinones (Biginelli-type product). However, regioselective catalysis³⁰ can be employed to enhance the selectivity of a particular product. Normally, the Hantzsch-type is favoured over the Biginelli-type product due to the higher electrophilic character of C4 as compared to N2. In our case, we found that nickel nanoparticles were an ideal catalyst for the regioselective synthesis of pyrazoloquinolinones (Hantzsch-type product) from substituted aminopyrazole. Proposed mechanisms for the synthesis of **5c** and **6a** are shown in Fig. 7 and 8 respectively. Basically the mechanisms of formation of triazoloquinazolinone and pyrazoloquinolinone

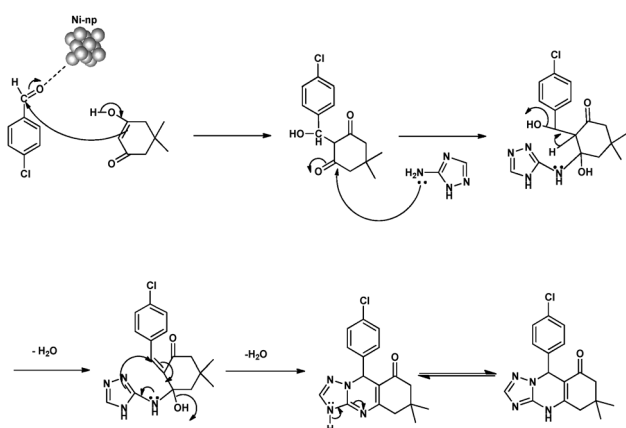


Fig. 7 Proposed mechanism for the synthesis of **5c**.

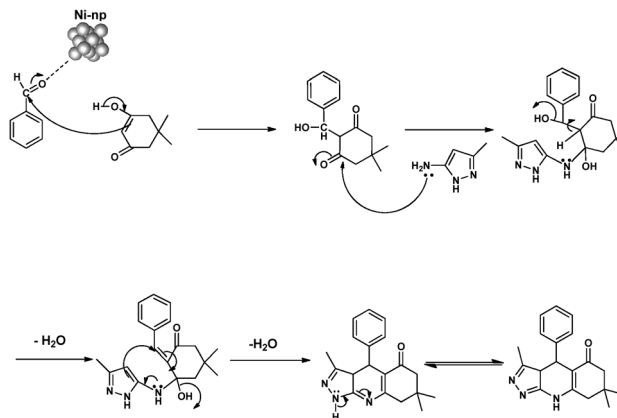


Fig. 8 Proposed mechanism for the synthesis of **6a**.

derivatives are similar but regioselectivity plays a role in the formation of pyrazoloquinolinones and hence, cyclisation occurs through carbon and not through nitrogen. All the derivatives which were synthesized are shown in Table 1.

The formation of the desired product was confirmed from the melting point data, infra-red, mass spectra and ¹H-NMR & ¹³C-NMR spectra. The IR spectrum of **5c** showed absorption peaks at 3436 cm^{-1} which corresponds to -NH stretching. The carbonyl absorption peak appeared at 1649 cm^{-1} which was much lower than expected but can be attributed to the delocalization of C=O . Another absorption peak at 618 cm^{-1} was observed, which corresponds to C-Cl stretching.

The ¹H-NMR spectrum of **5c** displayed two singlets at 0.705 ppm and 0.788 ppm which are due to the six methyl protons on the third ring. A singlet at 10.94 ppm was also observed, which can be correlated to the bridging -NH proton. In the ¹³C spectrum of **5c** we observed a peak at 192.98 ppm which can be correlated to the presence of carbonyl carbon. Another important peak was observed at 57.34 ppm which corresponds to the methine carbon of the desired product *i.e.* **5c**. The mass spectrum of **5c** exhibited a molecular ion peak at m/z 328 (M^+) which further corroborated the formation of **5c**. The XRD analysis of a single crystal of **5c** gave final confirmation of the formation of the desired product.

The IR spectrum of **6a** showed absorption peaks at 3237 cm^{-1} which corresponds to -NH stretching. The carbonyl absorption peak appeared at 1590 cm^{-1} , which was much lower than expected, but can be attributed to the delocalization of C=O . The ¹H NMR spectrum of **6a** displayed two singlets at 0.696 ppm and 0.757 ppm which are due to the six methyl protons on the third ring. A singlet at 11.484 ppm was also observed which can be correlated to the bridging -NH proton. The ¹³C-NMR spectrum of **6a** displayed a peak at 192.78 ppm which clearly indicated the presence of a carbonyl carbon. Another peak at 35.08 ppm validated the presence of the methine carbon. The mass spectrum of **6a** exhibited the molecular ion peak at m/z 307 (M^+) which suggested the formation of **6a**. Finally, from the XRD analysis of a single crystal of **6a**, we were able to confirm affirmatively that the desired product was synthesized.

Table 1 Synthesis of compounds 5a–h and 6a–j

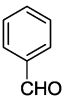
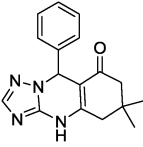
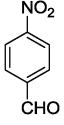
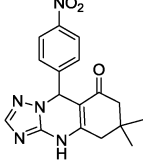
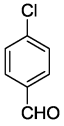
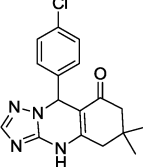
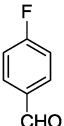
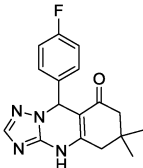
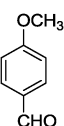
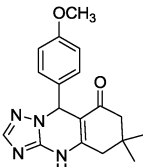
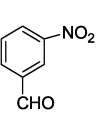
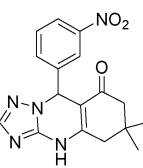
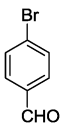
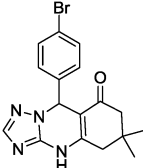
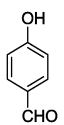
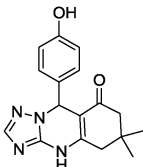
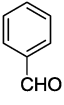
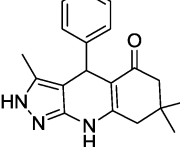
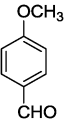
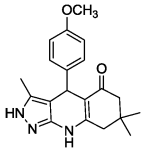
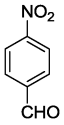
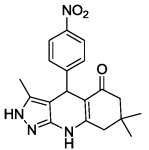
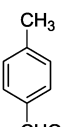
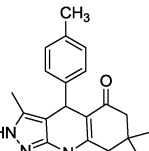
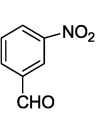
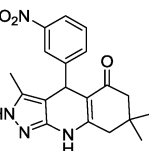
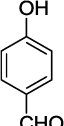
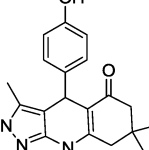
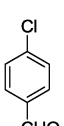
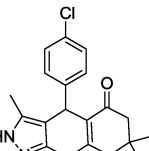
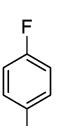
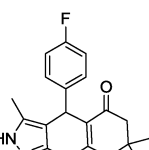
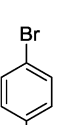
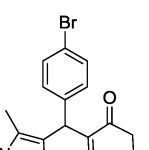
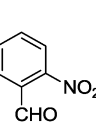
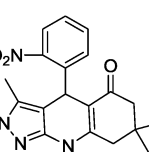
Compound	Aldehyde	Product	Time/min	Yield (%)	Appearance	Mp (found)/°C
5a			10	90	Light yellow crystal	249–251
5b			10	93	Pale yellow crystal	301–302
5c			10	92	Pale yellow crystal	297–298
5d			10	90	Colourless crystal	303–305
5e			10	88	Colourless crystal	230–232
5f			10	85	Pale yellow solid	290–292
5g			10	91	Yellow crystal	282–285
5h			10	89	Pale yellow solid	303–304
6a			10	96	Colourless crystal	230–232

Table 1 (continued)

Compound	Aldehyde	Product	Time/min	Yield (%)	Appearance	Mp (found)/°C
6b			10	95	Yellowish solid	295–297
6c			10	98	Pale yellow crystal	300–302
6d			10	94	Pale yellowish crystal	310–312
6e			10	93	Yellow crystal	298–300
6f			10	95	Light pinkish solid	272–275
6g			10	97	Colourless crystal	305–307
6h			10	96	Colourless crystal	338–340
6i			10	96	Colourless crystal	315–317
6j			10	91	Yellow solid	262–265

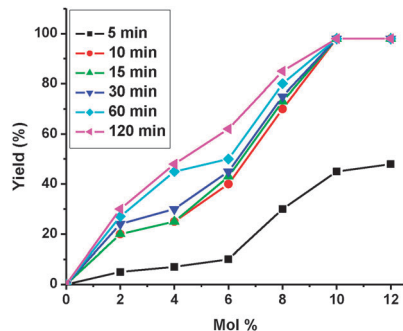


Fig. 9 Optimization of catalyst loading with respect to yield of **6c**.

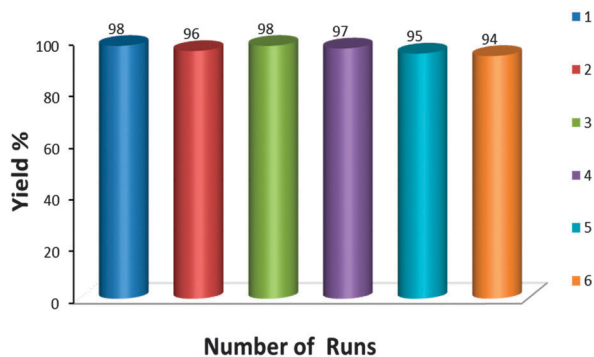


Fig. 10 Reusability plot of nickel nanoparticles.

Catalyst optimization

A series of tests were performed to standardize the optimum quantity of nickel nanoparticle required for the chemical condensation concerned (Scheme 1), and 10 mole percent was found to be the ideal amount. Another set of tests were performed to optimize the time of reaction, and 10 minutes was concluded to be the ideal time. The optimization plot for catalyst loading and reaction time is shown in Fig. 9.

In order to study the reusability of the catalyst, several re-runs were performed for the synthesis of **6c** using recycled nickel nanoparticles and it was found that the yield of the desired product (*i.e.* **6c**) was not significantly affected till the sixth cycle (as shown in Fig. 10). A slight decrease can be observed, however, which can be attributed to the aggregation of the nanoparticles, as is evident from the TEM images (Fig. 2). The process of recycling the nanoparticles was carried out in a very simple and easy manner. It involves recovery of the nanoparticles from the reaction mixture on completion of the synthesis process using an ordinary magnet. They were then thoroughly washed with acetone and Millipore water and allowed to dry. After drying, they were reused again as a catalyst.

X-Ray crystallography

The single crystal X-ray diffraction (XRD) data were collected at 293 K with Mo K α radiation ($\lambda = 0.71073 \text{ \AA}$) using an Agilent Xcalibur (Eos, Gemini) diffractometer equipped with a graphite monochromator. The software used for data collection CrysAlis

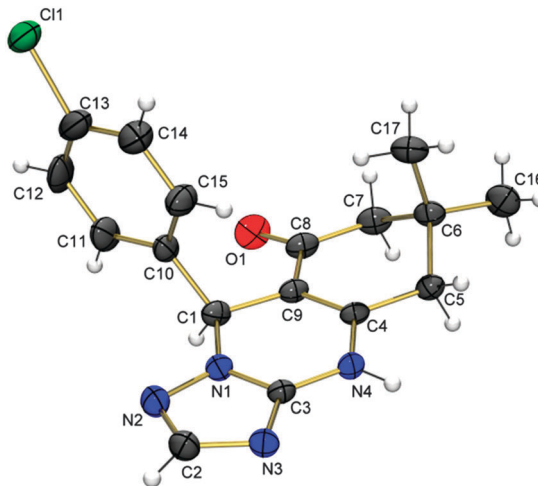


Fig. 11 ORTEP image of **5c** (CCDC 1024257).

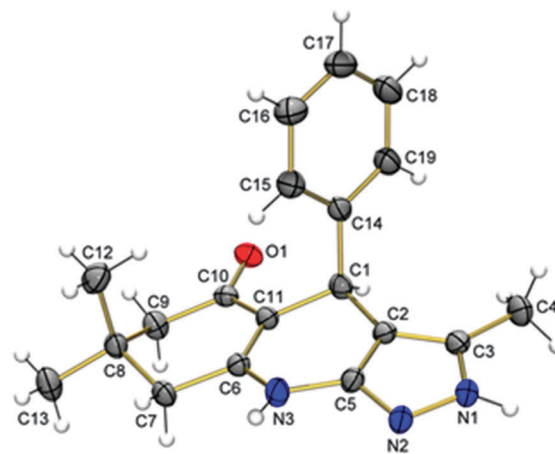


Fig. 12 ORTEP image of **6a** (CCDC 1024256).

PRO (Agilent, 2011), data reduction CrysAlis PRO and cell refinement CrysAlis PRO. The structures were solved by direct methods and refined by Olex2.refine. ORTEP images of **5c** and **6a** are shown in Fig. 11 and 12.

Conclusion

The utility of nickel nanoparticles in the catalysis of Hantzsch and Biginelli type reactions have been successfully demonstrated under short reaction time conditions. Through our approach we have opened up a wider scope for nickel nanoparticles in regioselective catalysis and the formation of C–N bonds.

Experimental

All the chemicals involved in the synthesis were purchased from Alfa Aesar, Sigma Aldrich & Merck and were used without further purification. The purity of the products were confirmed by infrared (IR), $^1\text{H-NMR}$, $^{13}\text{C-NMR}$ and mass spectra besides

X-ray diffraction (XRD) and melting point data. Melting points were determined in open capillary tubes and are uncorrected. IR spectra were recorded in KBr pellets on a Perkin Elmer Spectrum 400 FTIR instrument, and the frequencies are expressed in cm^{-1} . $^1\text{H-NMR}$ and $^{13}\text{C-NMR}$ spectra were recorded on a Bruker Avance II-400 spectrometer in DMSO-d_6 (chemical shifts in δ with TMS as internal standard). Mass spectral data were obtained with a JEOL D-300 (ESI) mass spectrometer. Single crystal XRD data were obtained with an Xcalibur-Eos-Gemini instrument and powder XRD analysis was conducted with an X'Pert Pro instrument. All reactions were monitored by thin layer chromatography (TLC) using precoated aluminum sheets (silica gel 60 F 254 0.2 mm thickness) and developed in an iodine chamber.

The TEM images were captured using a transmission electron microscope of JEM-2100 make, 200 kV (JEOL) and SEM and EDAX imaging were carried out with scanning electron microscope of JSM-6360 (JEOL) make.

General procedure for preparation of 5a–h, 6a–j

In a 50 ml round bottom flask, 3-amino-1*H*-1,2,4-triazole/3-amino-5-methyl-1*H*-pyrazole (1 mmol), aldehyde (1 mmol), dimedone (1 mmol) and nickel nanoparticle (10 mol%) were refluxed in acetonitrile (10 ml) for 10 minutes. On cooling, solid crystals separated out. The nickel nanoparticles were retrieved magnetically and the reaction mixture was filtered. The residue was dried and analysed.

Spectral data of selected compounds

6,6-Dimethyl-9-phenyl-5,6,7,9-tetrahydro-[1,2,4]triazolo[5,1-*b*]quinazolin-8(4*H*)-one (5a). IR (KBr): 3445, 2962, 1650, 1594, 1374, 1252, 721 cm^{-1} . $^1\text{H NMR}$ (DMSO-D_6 , 400 MHz): δ 11.14 (s, 1H), 7.68 (s, 1H), 7.17–7.29 (m, 5H), 6.19 (s, 1H), 2.52–2.59 (m, 2H), 2.19 (d, $J = 16$ Hz, 1H), 2.05 (d, $J = 16$ Hz, 1H), 1.03 (s, 3H), 0.95 (s, 3H). $^{13}\text{C NMR}$ (DMSO-D_6 , 100 MHz): δ 26.77, 28.45, 32.16, 49.74, 57.89, 105.55, 126.92, 127.69, 128.23, 141.55, 146.82, 150.24, 150.39, 192.96. ESI-MS: m/z 295 $[\text{M} + \text{H}]^+$.

3,7,7-Trimethyl-4-(4-nitrophenyl)-6,7,8,9-tetrahydro-2*H*-pyrazolo[3,4-*b*]quinolin-5(4*H*)-one (6c). IR (KBr): 3262, 3068, 2952, 1593, 1547, 1255, 740 cm^{-1} . $^1\text{H NMR}$ (DMSO-D_6 , 400 MHz): δ 11.61 (s, 1H), 9.63 (s, 1H), 7.82 (d, $J = 8$ Hz, 2H), 7.14 (d, $J = 8$ Hz, 2H), 4.84 (s, 1H), 2.18–2.21 (m, 2H), 1.86 (d, $J = 16$ Hz, 1H), 1.68 (d, $J = 16$ Hz, 1H), 1.62 (s, 3H), 0.75 (s, 3H), 0.68 (s, 3H). $^{13}\text{C NMR}$ (DMSO-D_6 , 100 MHz): δ 9.28, 26.89, 28.86, 31.90, 35.46, 40.92, 50.22, 102.51, 105.89, 123.19, 128.38, 135.39, 145.19, 146.05, 153.34, 155.89, 192.81. ESI-MS: m/z 353 $[\text{M} + \text{H}]^+$.

Acknowledgements

The authors would like to thank UGC for financial assistance in the form of a fellowship, SAIF-NEHU, SAIF-CIL-Punjab University and the Department of Chemistry, NEHU for analytical assistance.

Notes and references

- (a) T. Zeng, W. W. Chen, M. C. Cirtiu, A. Moores, G. Song and C.-J. Li, *Green Chem.*, 2010, **12**, 570–573; (b) M. M. Mojtahedi, M. S. Abaee and T. Alishiri, *Tetrahedron Lett.*, 2009, **50**, 2322–2325.
- A. Saxena, A. Kumar and S. Mujumdar, *J. Mol. Catal. A: Chem.*, 2007, **269**, 35–40.
- W. Zhang, H. Qi, L. Li, X. Wang, J. Chen, K. Peng and Z. Wang, *Green Chem.*, 2009, **11**, 1194–1200.
- F. Alonso, P. Riente and M. Yus, *Synlett*, 2007, 1877–1880.
- (a) F. Alonso, P. Riente and M. Yus, *Synlett*, 2008, 1289–1292; (b) F. Alonso, P. Riente and M. Yus, *Tetrahedron*, 2008, **64**, 1847–1852; (c) F. Alonso, P. Riente and M. Yus, *Tetrahedron Lett.*, 2008, **49**, 1939–1942.
- V. Polshettiwar, B. Baruwati and R. S. Varma, *Green Chem.*, 2009, **11**, 127–131.
- A. Dhakshinamoorthy and K. Pitchumani, *Tetrahedron Lett.*, 2008, **49**, 1818–1823.
- F. Alonso, P. Riente and M. Yus, *Synlett*, 2009, 1579–1582.
- L. Zank and J. Zielinski, *Appl. Catal., A*, 2008, **334**, 268–276.
- (a) V. Nair, C. Rajesh, A. Vinod, U. S. Bindu, A. R. Streekenh, S. Mathen and L. Balagopal, *Acc. Chem. Res.*, 2003, **36**, 899–907; (b) D. J. Ramon and M. Yus, *Angew. Chem., Int. Ed.*, 2005, **44**, 1602–1634; (c) A. Domling, *Chem. Rev.*, 2006, **106**, 17–89; (d) A. Domling and I. Ugi, *Angew. Chem., Int. Ed.*, 2000, **39**, 3168–3210; (e) J. Zhu and H. Bienaymé, *Multi-component Reactions*, Wiley-VCH, Weinheim, 2005; (f) R. W. Armstrong, A. P. Combs, P. A. Tempest and S. D. Brown, *Acc. Chem. Res.*, 1996, **29**, 123–131.
- (a) K. C. Liu and M. K. Hu, *Arch. Pharm.*, 1986, **319**, 188–189; (b) S. K. Pandey, A. Singh and Nizamuddin, *Eur. J. Med. Chem.*, 2009, **44**, 1188–1197; (c) G. F. Yang, R. F. Lu, X. N. Fei and H. Z. Yang, *Chin. J. Chem.*, 2000, **18**, 435–440.
- V. Alagarsamy, R. Revathi, S. Meena, K. V. Ramaseshu, S. Rajasekaran and C. E. De, *Indian J. Pharm. Sci.*, 2004, **66**, 459–462.
- V. Alagarsamy, G. Murugananthan and R. Venkateshperumal, *Biol. Pharm. Bull.*, 2003, **26**, 1711–1714.
- V. Alagarsamy and U. S. Pathak, *Bioorg. Med. Chem.*, 2007, **15**, 3457–3462.
- V. Alagarsamy, *Pharmazie*, 2004, **59**, 753–755.
- Y. Xia, Z. Y. Yang, M. J. Hour, S. C. Kuo, P. Xia, K. F. Bastow, Y. Nakanishi, P. Nampoothiri, T. Hackl, E. Hamel and K. H. Lee, *Bioorg. Med. Chem. Lett.*, 2001, **11**, 1193–1196.
- M. J. Hour, L. J. Huang, S. C. Kuo, Y. Xia, K. Bastow, Y. Nakanishi, E. Hamel and K. H. Lee, *J. Med. Chem.*, 2000, **43**, 4479–4487.
- (a) E. M. Aboul-Fetouh, A. A. Ashraf, H. F. Hassan and A. B. Eman, *Beilstein J. Org. Chem.*, 2007, **3**, 11; (b) V. V. Lipson, N. V. Svetlichnaya, V. V. Borodina, M. G. Shirobokova, S. V. Shishkina, O. V. Shishkin and V. I. Musatov, *Russ. J. Org. Chem.*, 2010, **46**, 1388–1398.
- G. Krishnamurthy and K. V. Jagannath, *J. Chem. Sci.*, 2013, **125**, 807–811.

- 20 R. G. Puligoundla, S. Karnakanti, R. Bantu, N. Kommu, S. B. Kondra and L. Nagarapu, *Tetrahedron Lett.*, 2013, **54**, 2480–2483.
- 21 M. M. Heravi, L. Ranjbar, F. Derikvand, B. Alimadadi and H. A. Oskooie, *Mol. Diversity*, 2008, **12**, 181–185.
- 22 P. K. Sahu, P. K. Sahu, R. Jain, R. Yadav and D. D. Agarwal, *Catal. Sci. Technol.*, 2012, **2**, 2465–2475.
- 23 Bristol-Meyers Co., *Fr. Demande*, 1973, **2**, 275; *Chem. Abstr.*, 1973, **79**, 78784n.
- 24 (a) A. M. Farghaly, N. S. Habib, M. A. Khalil and O. A. El-Sayed, *Alexandria J. Pharm. Sci.*, 1989, **3**, 90–94; (b) A. M. Farghaly, N. S. Habib, M. A. Khalil and O. A. El-Sayed, *Chem. Abstr.*, 1990, **112**, 7420b.
- 25 (a) R. R. Crenshaw, G. M. Luke and P. Smirnov, *J. Med. Chem.*, 1976, **19**, 262–275; (b) P. Smirnov and R. R. Crenshaw, *Antimicrob. Agents Chemother.*, 1977, **11**, 571–573; (c) P. Smirnov and R. R. Crenshaw, *Chem. Abstr.*, 1977, **85**, 153844d; (d) R. R. Crenshaw, G. M. Luke and P. Smirnov, *Can. Pat.*, 1978, **10**, 538; *Chem. Abstr.*, 1978, **89**, 179995r.
- 26 R. Gein Stein, J. H. Biel and T. Singh, *J. Med. Chem.*, 1970, **13**, 153–155.
- 27 M. R. Bell and J. H. Ackerman, US Pat., 4,920,128, 1990; *Chem. Abstr.*, 1990, **113**, 172015b.
- 28 F. Gatta, M. Pomponi and M. Marta, *J. Heterocycl. Chem.*, 1991, **28**, 1301–1307.
- 29 Z. G. Wu, M. Munoz and O. Montero, *Adv. Powder Technol.*, 2010, **21**, 165–168.
- 30 T. N. Glasnov and C. O. Kappe, *Org. Synth.*, 2009, **86**, 252–261.